PHYSICAL REVIEW A VOLUME 18, NUMBER 4 OCTOBER 1978

Motional-Stark-effect-induced anticrossings

G. C. Neumann,* B. R. Zegarski, and Terry A. Miller
Bell Laboratories, Murray Hill, New Jersey 07974

M. Rosenbluh, R. Panock, and B. Lax
Francis Bitter National Magnet Laboratory and Physics Department, Massachusetts Institute of Technology, Cambridge, Massachusetts 02139

(Received 22 February 1978)

Atoms moving through a magnetic field suffer a Stark effect whose magnitude is dependent upon the atom's velocity. This velocity-dependent perturbation has recently been exploited as a Doppler narrowing technique, and in this paper we consider atomic anticrossings induced by it. Experimentally such anticrossings are observed between $n\,^3D - n\,^{1,3}F$ states of He for $n = 4$–9, with $n = 8$ being considered in detail. Theoretical expressions are derived for motional-Stark-effect-induced anticrossing line shapes. Good agreement with the observed line shapes is obtained and the theoretical analysis allows a value of the $n\,^3D - ^{1,3}F$ interval to be obtained which is in good agreement with previous predictions.

I. INTRODUCTION

In a recent paper[1] on CO_2-laser-induced transitions between different Rydberg levels of He, it was found that the motional electric field, experienced by an atom moving in a magnetic field, could strongly modify the normal Doppler-broadened line shape. It was shown that the interaction of the two velocity-dependent terms, Doppler and motional-Stark, could lead to a new line shape with a very sharp cutoff. Indeed the slope of this cutoff was effectively determined by the homogeneous, not Doppler, linewidth, and thus one obtains a novel technique for sub-Doppler spectroscopy.

Rydberg levels of the He atom have also been the site of another relatively new spectroscopic technique, that of anticrossing spectroscopy.[2-8] In these experiments pairs of He Rydberg levels are magnetically tuned to near degeneracy. However, because of the existence of a perturbation between pairs of levels, the levels do not actually cross but go through an avoided crossing or anticrossing. The presence of an anticrossing at a specific magnetic field is detected by a (complementary) change in the optical emission from one or both levels.

Anticrossings can generally be divided into two broad categories[9] based upon whether the perturbation is external (such as an applied field) or internal (such as spin-orbit coupling). The latter or internal sort have been exploited to measure $n\,^1D$-^3D separations for $n = 3$–20 in He.[2,5,7] These have been very useful in determining singlet-triplet separations as well as the strength of the spin-orbit coupling between ^1D and ^3D states. Nonetheless, the accuracy of these experiments has primarily been limited by the relatively broad anticrossing signals obtained. The width of the anticrossing in this case is determined by the strength of the spin-orbit coupling which is clearly beyond the ability of the experimenter to control. Moderate progress towards the resolution of this problem has been made by the introduction of a mixed type of experiment[8,9] where the pair of levels are ultimately coupled in higher order by a combination of spin-orbit and external field perturbations.

Likewise, purely external electric-field-induced anticrossing experiments have long been known,[9] particularly with He^+ and H. External electric-field-induced anticrossings have a certain appeal in that their widths are, to a degree, at the control of the experimenter, for he has the ability to control the external electric field strength. However, the anticrossing lines cannot be sharpened continually by reducing the external electric field to zero for, among other reasons, the atom will always see the motional-Stark field generated by its motion through the magnetic field.

Since the motional field is the minimum electric field (for a given velocity or temperature and magnetic field) obtainable, it seems appropriate to try to perform anticrossing experiments utilizing it. This idea becomes even more intriguing when one realizes the analogy with the sub-Doppler laser experiments recently reported.[1] The anticrossing can be thought of as the zero-frequency limit of this experiment. Even though at zero frequency there is no Doppler broadening, the anticrossing can be quite wide if the perturbation is strong. On the other hand, atoms with zero velocity perpendicular to the magnetic field ($v_\perp = 0$) will have zero perturbation and, neglecting lifetime broadening, zero width. However, they also have zero intensity. Nonetheless, we will show that the intensity rises very rapidly with increasing perturbation strength (velocity) and anticrossing signals of near-maximum intensity may be obtained for

widths only slightly more than that required by the uncertainty principle. The resulting line shape, obtained by including atoms of all velocities, may well be expected to be similar to that obtained in the laser experiments, i.e., one characterized by a relatively sharp cutoff and a long exponential tail.

It is appropriate to mention that anticrossings have been previously observed[10,11] in H where the perturbation was due to the electric field generated by motion through a magnetic field. However, these experiments were rather different in spirit from our observations on thermal atoms. The H was formed by dissociation of H_2. The partitioning of the dissociation energy into kinetic energy was measured from the width (and hence the atom's velocity) of the observed anticrossing.

The purpose of our work is to explore both theoretically and experimentally the motional-Stark-effect-induced anticrossing line shape. The remainder of this paper is divided as follows. Section II is a short description of our apparatus. Section III is divided into two parts. Section III A describes spectroscopically the levels involved in the anticrossing and our motivation for choosing these levels. Section III B consists of a detailed theory of the expected line shape. Section IV compares the experimental results with the computed ones.

II. EXPERIMENTAL

The low n anticrossings were observed with the anticrossing apparatus at the Francis Bitter National Magnet Laboratory at MIT. The higher n anticrossings were observed with the apparatus at Bell Laboratories. In both apparatuses, the He states were excited by a controlled beam of electrons (~100 V). The appropriate $n\,^3D$ emission line was selected by a monochrometer and the intensity measured as a function of field. Efforts were made to keep pressure low (<15 mTorr) and electron-gun currents low (<1 mA) to avoid stray electric fields from space charge. Details of the apparatuses can be found elsewhere.[3,5]

III. THEORY

A. Spectroscopic analysis

In order for an electric field to couple a pair of atomic levels in second order, the levels must differ in L by 1. In terms of magnetic tunability and ease of observability of optical emission, the obvious choice for these anticrossing experiments are the n D-F anticrossings. The selection rules for an allowed anticrossing for a perpendicular electric field (as the motional field is) are $\Delta M_L = \pm 1$ and hence occur with an effective g value $g_e = \sim 1$. An example of this kind of anticrossing is marked with the solid circle at high field in Fig. 1.

As we were able to confirm experimentally, these anticrossings are rather unsuitable for our purpose. The reason for this is rather simple. Consider as an example the $n=8$ ^3D-^3F anticrossing, which using Mac Adam and Wing's results,[12] should occur at ≈22 kG. A He atom moving at rms velocity in this magnetic field would see an electric field of ≈25 V/cm. For the $n=8$ ^3D-^3F transition this corresponds to a linewidth of over 4 kG, hardly a narrow line. The dipole matrix element, of course, decreases for smaller n; however, the magnetic field at which the anticrossing occurs increases in a roughly, although not precisely, compensating fashion. Thus for all n, the allowed ($g_e \approx 1$) D-F anticrossings are quite broad.

This problem can be overcome for the triplet states by going to a different pair of levels. Consider as an example the levels ^3D, $M_s=1$, $M_L=0$ and ^3F, $M_s=0$, $M_L=0$ (or equivalently ^3D, $M_s=0$, $M_L=0$ and ^3F, $M_s=-1$, $M_L=0$) which converge with an effective $g_e \approx 2$. The anticrossings between these levels are indicated by solid dots in Fig. 1. In the decoupled limit no electric-field-induced anticrossing can exist between them as $\Delta M_s = 1$. However, at finite magnetic field, one must take into account fine-structure mixing. For instance, the level ^3D, $M_s=1$, M_L is actually $|^3D, M_s=1, M_L\rangle + a\,|^3D, M_s=0, M_L+1\rangle$. (In a similar way, but considerably less so, the ^3F levels are not pure.) The coefficient a in the above example is given by

$$a = \frac{\langle {}^3D, M_s=1, M_L | \hat{H}_{FS} | {}^3D, M_s=0, M_L+1\rangle}{\mu_0 H}.$$

The fine-structure Hamiltonian $\hat{H}_{FS}$ has been given previously[2] and contains the spin-orbit and spin-

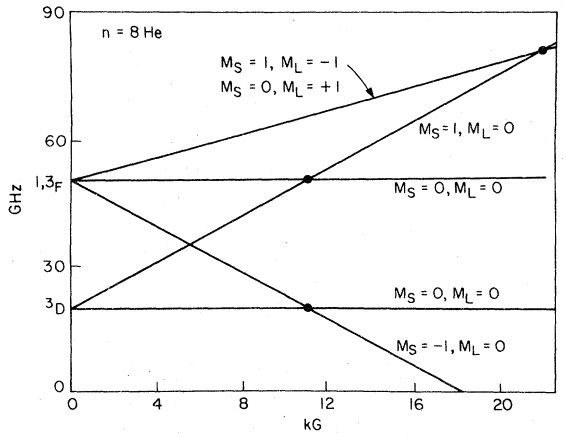

FIG. 1. Positions of "full-field" and "half-field" anticrossings between the $n=8$ ^3D and $n=8$ $^{1,3}F$ levels of helium.

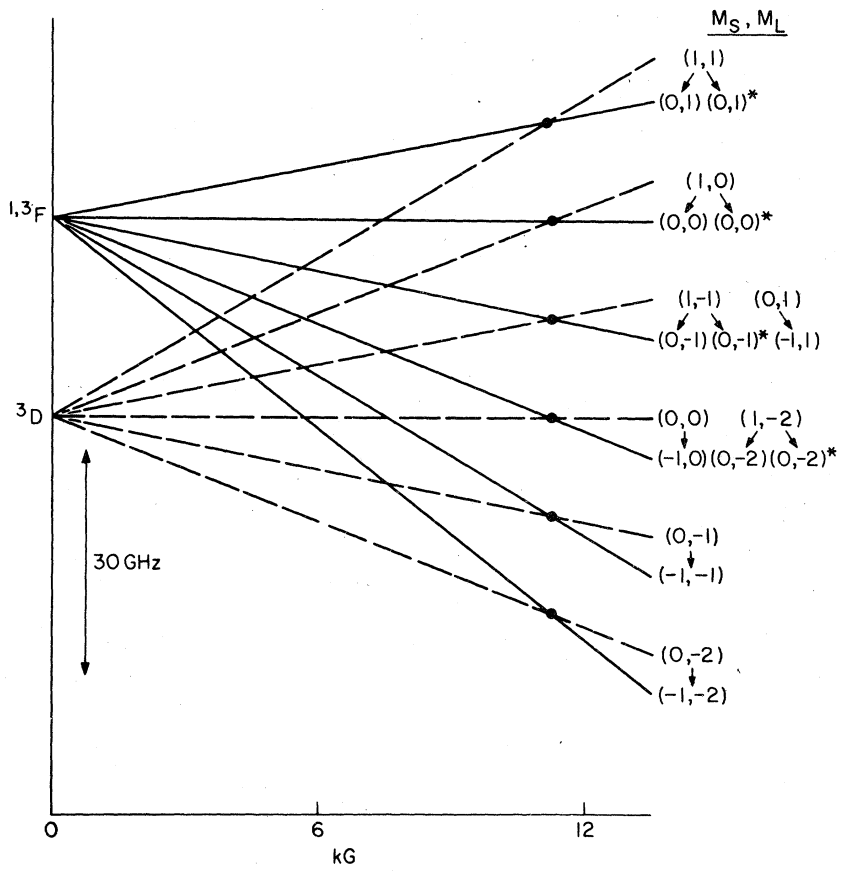

FIG. 2. "Half-field" anticrossings between the $n = 8$ ^3D and the $n = 8$ $^{1,3}F$ state. The values of M_L and M_S involved in the anticrossing are indicated, and the anticrossing sublevels emanating from the ^1F state are starred. The figure assumes complete degeneracy between the ^1F and ^3F levels. The arrows indicate the pairs of levels between which the anticrossings occur.

spin parameters. Using hydrogenic values for these parameters for $n = 8$ and the predicted field of ≈11 kG, one finds an (M_L-dependent) value for a of 10^{-2}–10^{-3}. Since the perturbation strength between the nominal ^3D, $M_s = 1$, M_L and ^3F, $M_s = 0$, M_L is just a times the previously calculated perturbation of 4-kG linewidth, we predict an anticrossing width of order 10–100 G.

The positions of the anticrossings are illustrated in Fig. 1. While there are only two distinct "half-field" anticrossings indicated, there are in reality 12 separate pairs of levels anticrossing. Figure 2 shows the complexity of the actual situation. As indicated in the figure there are eight anticrossings with $\Delta M_s = 1$ and $\Delta M_L = 0$. These anticrossings occur between sublevels of the ^3D and ^3F levels. What is more, the ^1F and ^3F states are known to be fairly strongly mixed[13] so that four more pairs of sublevels of the ^1F and ^3D levels may anticross. One should note that the positions of all the anticrossings may not be completely degenerate, and that no $^3D, M_L = 2$ sublevel can anticross because the required fine-structure mixing cannot take place.

B. Line-shape analysis

In Sec. III B we discussed the various interactions of an atom moving in a magnetic field with given velocity $v_\perp$. In this section we wish to average over all atoms in the ensemble to obtain the overall line shape. This observed motional-Stark-effect-induced line shape is obtained by convoluting a probability distribution $I_i(H' - H_0)$ for having an atom with anticrossing centered at H' (H_0 is the anticrossing position for an atom with $v_\perp = 0$), with $I_h(H - H')$ the anticrossing line shape of the atom centered at H'. If $I(H)$ is the final line shape, then

$$I(H) = \int_{-\infty}^{+\infty} I_h(H - H') I_i(H' - H_0)\, dH'. \tag{1}$$

The probability distribution I_i is obtained by considering a Boltzmann distribution of velocities with the restriction that the frequency shift $\delta\omega$ and the related field shift are given by the Stark-field perturbation in second order,

$$\delta\omega = 2\pi g_e \mu_0 (H - H_0) = (\alpha H_0^2 / c^2) v_\perp^2, \tag{2}$$

where

$$\alpha = \hbar^{-1}\left(\sum_m \frac{(\mu_\perp^m)^2}{\Delta E_{mn}} - \sum_{m'} \frac{(\mu_\perp^{m'})^2}{\Delta E_{m'n}}\right). \tag{3}$$

Then α is a Stark coupling coefficient for the two levels m and m' involved in the transition. The first term of α gives the Stark shift in second order of the mth (upper) level while the last term gives the second order shift of the m'th (lower) level. In the above $\vec{H}$ defines the z direction with $\nu_\perp^2 = \nu_x^2 + \nu_y^2$, the effective Stark field arising from $\vec{v}\times\vec{H}/c$. Finally, we have made the assumption that $H_0 \gg (H - H_0)$ in using H_0 rather than H in the final equality.

The atoms can be presumed to have a Maxwell-Boltzmann distribution in velocity space. What we require is the corresponding distribution $I_i(H' - H_0)$ in field space or the corresponding distribution $P(\delta\omega) = (2\pi g_e\mu_0)^{-1} I_i(H' - H_0)$ in frequency space. This can be obtained from the velocity distribution by multiplying it by a δ function which is nonzero for only those velocities satisfying Eq. (2). Thus we obtain

$$P(\delta\omega) = \frac{1}{\pi\nu_0^2}\int_{-\infty}^{\infty}\int_{-\infty}^{\infty} e^{-\nu_\perp^2/\nu_0^2}\,\delta\left(\frac{\alpha H_0^2}{c^2}\nu_\perp^2 - \delta\omega\right) d\nu_x\, d\nu_y, \tag{4}$$

where we have carried out the integration over ν_z, $\nu_0^2 = 2kT/M$, and c is the speed of light.

In order to carry out this integral it is useful to note that Eq. (2) can be written

$$\nu_x^2 = (r - \nu_y)(r + \nu_y), \tag{5}$$

with $r = (c/H_0)\sqrt{\delta\omega/\alpha}$. Since ν_x must be real it is clear that Eq. (2) restricts ν_y to values $-r \le \nu \le r$. Putting in this restriction and rewriting the argument of the δ function using Eq. (2) yields

$$P(\delta\omega) = \left(\frac{1}{\pi\nu_0^2}\right) e^{-c^2\delta\omega/\alpha H_0^2\nu_0^2} \times \int_{-r}^{r} d\nu_y \int_{-\infty}^{\infty} d\nu_x\,\delta[\eta\nu_x^2 - (\delta\omega - \eta\nu_y^2)], \tag{6}$$

where $\eta = \alpha H_0^2/c^2$.

It should be noted that Eq. (5) requires the quantity $\delta\omega/\alpha$ to be positive. Thus for $\alpha > 0$, $\delta\omega \ge 0$, and $\alpha < 0$, $\delta\omega \le 0$; otherwise $P(\delta\omega) = 0$. If one makes the substitution $u = (\alpha H_0^2/c^2)\nu_x^2$, the last integral can be integrated by recourse to standard formulas[14] for δ-function integrals. This yields

$$P(\delta\omega) = \left(\frac{1}{\pi\nu_0^2}\right) e^{-c^2\delta\omega/\alpha H_0^2\nu_0^2} \int_{-r}^{r} \left(\frac{c^2}{|\alpha| H_0^2}\right)^{1/2} \times (\delta\omega - \eta\nu_y^2)^{-1/2}\, d\nu_y \tag{7}$$

Performing the analytical integral in Eq. (7) and eliminating $\delta\omega$ in favor of $(H' - H_0)$ from Eq. (2) yields the final normalized result

$$I_i(H' - H_0) = \begin{cases} \dfrac{2\pi c^2 g_e\mu_0}{|\alpha| H_0^2\nu_0^2}\, e^{-c^2 g_e\mu_0 2\pi(H' - H_0)/\alpha H_0^2\nu_0^2}, & \dfrac{(H' - H_0)}{\alpha} \ge 0 \\ 0, & \dfrac{(H' - H_0)}{\alpha} < 0. \end{cases} \tag{8}$$

To complete the problem we must convolute the anticrossing line shape $I_h(H - H')$. Using the standard formula for anticrossing line shape[2] we obtain

$$I_h(H - H') = \frac{-2\bar{\tau}^{-1}[\rho_a^0\tau_a - \rho_b^0\tau_b](K_a\tau_a - K_b\tau_b)|V_{ab}|^2}{4|V_{ab}|^2 f_\tau + \hbar^2/\bar{\tau}^2 + g_e^2\mu_0^2(H - H')^2}, \tag{9}$$

where

$$\tau^{-1} = \tau_a^{-1} + \tau_b^{-1}, \quad f_\tau = \tau_a\tau_b/\bar{\tau}^2,$$

and the rest of the symbols are as previously defined. The important point to note is that the perturbation V_{ab} between the anticrossing levels is not a constant over the imhomogeneously broadened linewidth. Rather, using Eq. (2) it can be written

$$|V_{ab}|^2 = \mu_{ab}^2\nu_\perp^2 H_0^2/c^2 = (g_e\mu_0\mu_{ab}^2 2\pi/\alpha)(H' - H_0), \tag{10}$$

where once again it has been assumed that $H_0 \gg (H' - H_0)$.

Combining Eqs. (8–10) according to Eq. (1) gives the motional-Stark-effect-induced anticrossing line shape,

$$I(H) = |B| \int_{H_0}^{\pm\infty} \frac{A(H' - H_0)e^{-B(H' - H_0)}}{2A(H' - H_0) + \hbar^2\tau^{-2} + g_e^2\mu_0^2(H - H')^2}\, dH', \tag{11}$$

where we have assumed for simplicity that $\tau_a = \tau_b$. The $\pm$ sign in the limit of the integral is chosen so that $(H' - H_0)/\alpha > 0$ for all values of the variable of integration. Physically, this means that the line shape will reverse field direction according to the sign of α. The constans A and B are defined by

$$A = 4\pi g_e\mu_0\mu_{ab}^2/\alpha \tag{12}$$

and

$$B = 2\pi c^2 g_e \mu_0 / \alpha H_0^2 \nu_0^2 . \quad (13)$$

IV. RESULTS

$^3D - {}^{1,3}F$ anticrossing spectra have been observed experimentally for $n = 4$–9. The $n = 4$–7 transitions have been observed at the MIT Francis Bitter National Magnet Laboratory, and the $n = 7$–9 transitions have been observed with the apparatus at Bell Laboratories. For several reasons, the theoretical and experimental work was focused on $n = 8$. The lower n are marked by partially resolved components. Unfortunately this resolution is incomplete and the numerous overlapping lines make line shape analysis difficult at best.

Theoretical estimates of the Stark asymmetry of the anticrossing line shapes indicate higher n are more asymmetric. By $n = 8$ the increasing Stark-effect strength, coupled with decreasing fine-structure interaction strength, leads to the situation of nearly complete degeneracy of the different M_L levels. High n's would, of course, approximate this situation even more perfectly; however, the signal-to-noise (SN) ratio becomes a problem. The $n = 9$ was easily observed and even higher n certainly could be observed, but $n = 8$ seems the best compromise for a high SN ratio and small nondegeneracy.

Figure 3 shows an experimental trace of the $n = 8$ $^3D - {}^{1,3}F$ anticrossing. This spectrum was observed at relatively low pressure and electron current. These steps were taken to minimize any stray inhomogeneous electric fields from space charge, etc. Runs at a current an order of magnitude higher did show distortion, with the high field "tail" becoming more pronounced. It is, of course, impossible to prove the absence of any distortion in the observed line shape, but it would appear to be minimal as the line shape was insensitive to small current and pressure changes in this low-current and low-pressure regime.

One can note that the observed line shape does indeed confirm our initial speculation. It is quite similar to the motional-Stark-effect line shapes in the laser magnetic resonance experiments with a relatively sharp cutoff and a long exponential tail. To simulate this line shape theoretically, one must turn to Eq. (11) and perform the numerical integration for the appropriate values of A, B, and τ. Finding values for A, B, and τ is relatively straightforward. The radiative lifetime τ is known[15,16] and was used. It is not totally certain that collisional shortening of τ is absent at these pressures but most likely it is not very great and the calculated line shape is not very sensitive to moderate changes in τ.

The values of A and B are slightly more difficult to calculate; they depend upon three physical parameters, α, μ_{ab}, and ν_0. The matrix element μ_{ab} gives the strength of the coupling between the D and F levels. As noted earlier, the anticrossings are only allowed via fine-structure mixing in the ^3D and ^3F states. Since this mixing is expected to be small in the ^3F states, and totally absent in the ^1F state, we will only include ^3D mixing. The mixing coefficient a, defined by Eq. (1), has been calculated using $n = 8$ ^3D fine structure constants. The value of μ_{ab} is then obtained by multiplying the hyrodgenic D-F transition moment by the M_L-dependent value of a.

In determining a in this manner, two other, probably partially canceling, effects are neglected. Fine-structure mixing between the ^3D and ^3G state is allowed via spin-spin interactions. This mixing would give a contribution to μ_{ab} from the G-F

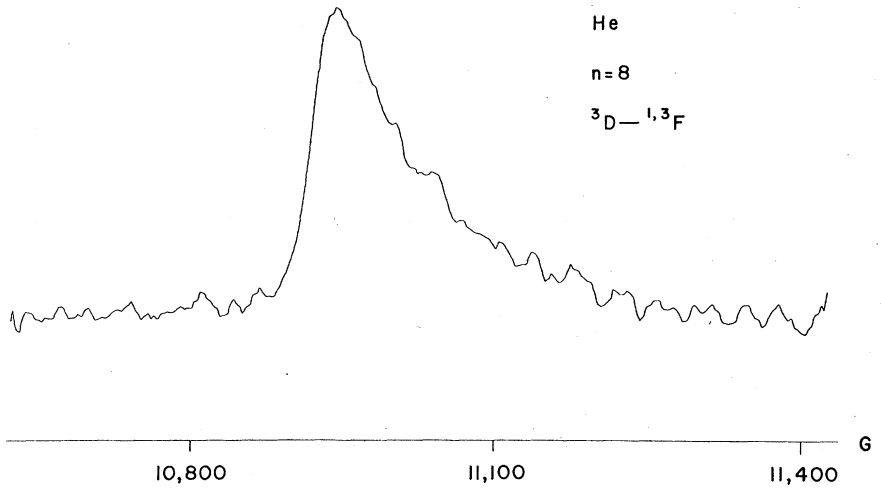

FIG. 3. Experimental trace of the $n = 8$ $^3D - {}^{1,3}F$ anticrossing. Light from the ^3D emission line was monitored and can be seen to increase at the anticrossing field. The experimental conditions included a pressure of ~10 mTorr, ~0.5 mA current, and ~20 min of averaging time.

transition moment. However, because both the mixing and the transition moments are likely to be smaller than those considered before, we neglect this effect. Another mixing effect that is present is the ^1F–^3F mixing, which would reduce μ_{ab} between either state but make both anticrossings allowed. Since the correct mixing coefficients are unknown, we neglect this correction. Because of these various unknown effects, μ_{ab} and A have considerable uncertainty. Fortunately, for values of μ_{ab} of the magnitude calculated, factor-of-2 variations cause only small effects in the line shape, and we are reasonably confident of the accuracy of μ_{ab} to this level.

The strength of the second-order Stark effect is given by α, which originates from a coupling of the F and D levels with other close lying levels. The calculation of α is involved but straightforward. In performing it we must consider the following levels: the Zeeman sublevels of the $^{1,3}G$ state that interact with Zeeman sublevels of the $^{1,3}F$ state with the same values of M_s (of course the ^1F and ^1G states have only those levels with $M_s = 0$) and the Zeeman sublevels of the $^{1,3}F$ level that interact with the Zeeman sublevels of the ^3D state with the same value of M_s.

For the example of the $^{1,3}F$, $M_s = 0$, $M_L = 0$ and ^3D, $M_s = 1$, $M_L = 0$ levels we have the following effects. The ^3D, $M_s = 1$ level is depressed by both the ^3F, $M_s = 1$, $M_L = \pm 1$ levels. For the $^{1,3}F$, $M_s = 0$, $M_L = 0$ level, the $^{1,3}G$, $M_s = 0$, $M_L = \pm 1$ have opposing effects but the net result is a small increase in the $^{1,3}F$ energy. The overall effect of the shifts in both states is to cause higher-velocity atoms to anticross at higher magnetic fields. Since α is field- and M_L-dependent, it varies for different transitions. However at the observed magnetic field, αE_0^2 is of the order of 100 MHz, where E_0 is the electric field seen by an atom with velocity v_0.

The final input necessary for determining A and B is the velocity v_0, which, of course, depends upon the system's temperature T. The observed line shape depends rather sensitively upon T. The value of T is not precisely known but it must rest within rather narrow limits. It cannot reasonably be below the ambiant 300°K but could be somewhat higher, since the excited He is very close to the electron gun, which is heated to ≈850°C. Rough considerations of heat transfer place the He gas temperature in the range of 300–500°K.

We see then that Eq. (11) is essentially predetermined except for a variable T, which is prescribed to lie within a narrow range. Thus each individual M_s M_L anticrossing line shape is well described. A problem arises, however, in that the observed line consists of up to 12 components. Furthermore, the relative intensity of the 12 components is not well determined because of uncertainties in possible alignment of M_L states by the excitation process and the unknown mixing in the ^1F and ^3F states. The precise positions of the M_L components are only roughly known, depending upon both fine-structure and quadratic Zeeman parameters.

In order to avoid an unmanageable situation both parametrically and computationally, we have resorted to a somewhat arbitrary treatment of the 12 components based upon the following considerations. (i) Figure 4 shows that different M_L (but independent of M_S) anticrossings have rather different appearances for the same input variables; thus it is necessary to include different M_L components. (ii) Calculations using the known fine-structure parameters and the $^{1,3}F$ intervals indicate that all the transitions have $\nu_\perp = 0$ centers within ≈25 G. Considering the overall width of the experimental trace in Fig. 3, while this nondegeneracy is not totally negligible, the line shape is not overly sensitive to its exact form. (iii) One can argue from an electrostatic collision model that one would expect that only the $M_s = 0$ components of the $^{1,3}F$ states are sufficiently populated to give the observed anticrossings. This statement follows from the fact that the ^1F state has only $M_s = 0$. The ^3F, $M_s = 0$ state is strongly mixed with the ^1F state and probably has a comparably high population. On the other hand, the $M_s = \pm 1$ ^3F levels are probably

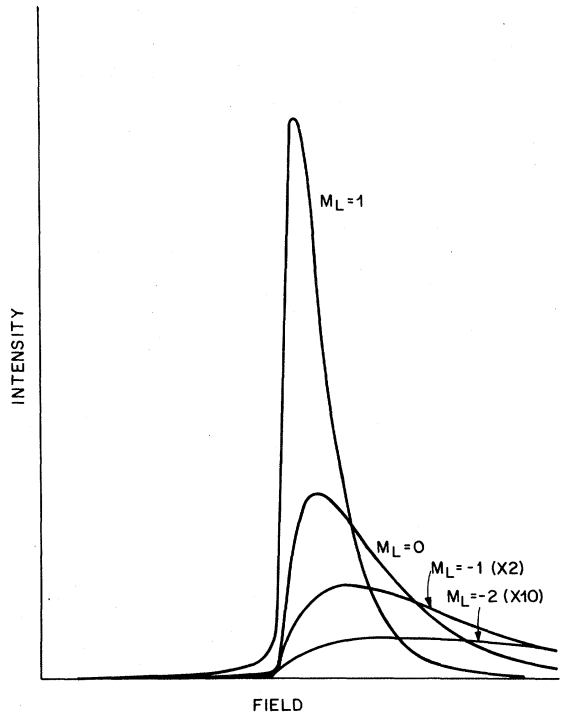

FIG. 4. Calculated line shapes for various M_L components involved in the $n = 8$ $^3D - {}^{1,3}F$ anticrossing.

poorly populated by collisions since the dominant interaction is electrostatic, which is ineffective in changing the quantum number M_s, M_s being well defined in high magnetic field.

Taking these considerations into account, we have approximated the 12-component convolution by a 4-component one. The four components are the 4 M_L anticrossings ^3D, $M_s=1 \leftrightarrow {}^1F$, $M_s=0$. The small relative shifts of the M_L lines are calculated from ^3D fine-structure data. It may be noted that overall shapes computed from other sets of components or all components differ only in the precise shifts assigned to individual M_L anticrossings. Small changes in these shifts have been shown by direct calculation not to alter significantly the overall line shape. Each of the four M_L comcomponents are assumed to have unit integral intensity. Putting the ^3F anticrossings at zero intensity is clearly an arbitrary solution to the problem of the relative intensities of the ^1F and ^3F states, for which no information is available.

The key virtue of the above assumptions is a calculation of easily manageable computational proportions and, most important, one free of any new parameters. Thus our line shape calculations have but one free parameter, the temperature, which is constrained to lie within a given range. Figure 5 shows a comparison of the line shape calculated for 450°K with an experimental trace. The agreement for this temperature was judged to be best and, interestingly, this is precisely the He temperature determined in a similar, but not identical, apparatus from the width of the Doppler profile.[1] Comparable calculations with the temperature raised or lowered by 50°C clearly gave inferior fits.

Overall, the agreement between computed and observed line shapes seems quite satisfactory. There is little doubt that the introduction of more components with variable intensity could give a perfect fit to experiment. However, little if anything of physical consequence would be obtained from this procedure.

The line shape fit also gives us a precise position for the intersection of the D and F curves for $v_\perp=0$ atoms. The value we find is $10\,892\pm16$ G, where the stated uncertainty is the standard deviation of seven measurements. Assuming a linear Zeeman effect this gives a zero-field interval of 30.524 ± 0.045 GHz. This value can be compared to the predicted $^3D_2-{}^1F_2$ and $^3D_2-{}^3F_2$ intervals from the power series of Mac Adam and Wing.[12] These values are, respectively, 30.576 and 30.472 GHz.

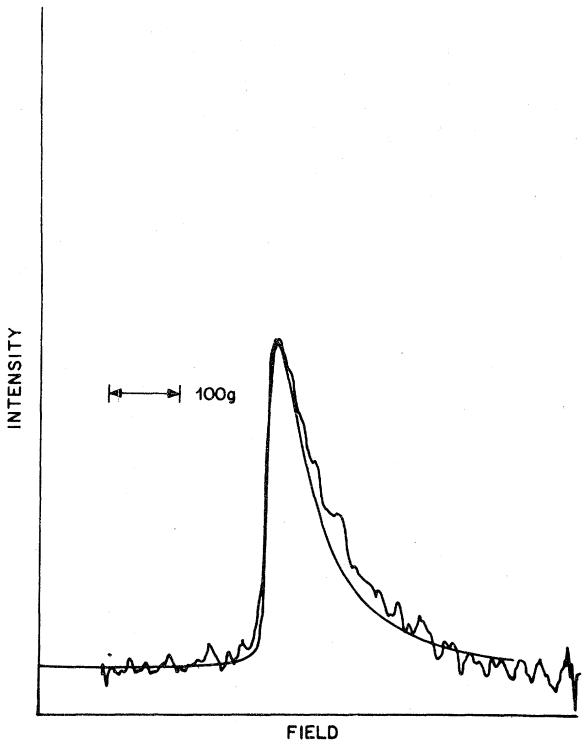

FIG. 5. Comparison between experimental anticrossing curve and one computed using the assumptions outlined in the text.

(One can also compare with the theoretical predictions of Chang and Poe[17] for $^3D_2-{}^{1,3}F_2$ of 30.12 GHz.) One can easily see that the present value falls very nearly between the two and we should certainly characterize the measured interval as $^3D-{}^{1,3}F$. However, the present error limits are sufficiently large, so that no real inference should be drawn as to the relative importance of the ^1F and ^3F anticrossings.

In summary, this paper reports the first observation of an anticrossing where the requisite perturbation is the thermal motional Stark field. A general theory is derived of anticrossings with a velocity-dependent perturbation of this sort. Experimentally, such anticrossings have been observed for the $n=4$–9 $^3D-{}^{1,3}F$ He states. The $n=8$ case has been examined in detail both experimentally and theoretically and good agreement between theory and experiment is obtained. The $n=8$ $^3D-{}^{1,3}F$ zero-field interval is derived from the anticrossing position and is in good agreement with the previous prediction for this interval.

*Present address: Dept. of Chemistry, Univ. of California, Berkeley, Calif. 94720.

[1]M. Rosenbluh, T. A. Miller, D. Larsen, and B. Lax, Phys. Rev. Lett. 39, 878 (1977).
[2]T. A. Miller and R. S. Freund, Adv. Magn. Reson. 9, 49 (1977).
[3]T. A. Miller, R. S. Freund, F. Tsai, T. J. Cook, and B. R. Zegarski, Phys. Rev. A 9, 2974 (1974).
[4]T. A. Miller, R. S. Freund, and B. R. Zegarski, Phys. Rev. A 11, 753 (1975).
[5]J. Derouard, R. Jost, M. Lombardi, T. A. Miller, and R. S. Fruend, Phys. Rev. A 14, 1025 (1976).
[6]H.-J. Beyer and K.-J. Kollath, J. Phys. B 8, L326 (1975).
[7]H.-J. Beyer and K.-J. Kollath, J. Phys. B 9 L185 (1976).
[8]H.-J. Beyer and K.-J. Kollath, J. Phys. B 10, L5 (1977); 11, 979 (1978).
[9]H.-J. Beyer and K. Kleinpopen, *Progress in Atomic Spectroscopy—Methods and Applications*, edited by W. Hanle and H. Kleinpoppen (Plenum, N.Y., 1978).
[10]L. Julien, M. Glass-Maujean, and J. P. Descoubes, J. Phys. B 6, L196 (1973).
[11]M. Glass-Maujean, Opt. Commun. 8, 260 (1973).
[12]K. B. Mac Adam and W. H. Wing, Phys. Rev. A 15, 678 (1977).
[13]K. B. Mac Adam and W. H. Wing, Phys. Rev. A 12, 1464 (1975).
[14]A. Messiah, *Quantum Mechanics* (North-Holland, Amsterdam, 1965).
[15]L. C. Green, N. C. Johnson, and E. K. Kolchin, Astrophys. J. 144, 369 (1966).
[16]R. T. Brown and J.-L. M. Cortez, Astrophys. J. 176, 267 (1972).
[17]T. N. Chang and R. T. Poe, Phys. Rev. A 10, 1981 (1974).